Hidden pathway for cytokine receptor activation: Structural insights into a marine sponge-derived lectin that activates the thrombopoietin receptor via recognition of the fucose moiety

Hiromi Watari[1]†, Hiromu Kageyama[2]†, Nami Masubuchi[3], Hiroya Nakajima[1], Kako Onodera[2], Pamela J. Focia[4], Takumi Oshiro[5], Takashi Matsui[5,6], Yoshio Kodera[5,6], Tomohisa Ogawa[2], Takeshi Yokoyama[2], Makoto Hirayama[7], Kanji Hori[7], Douglas M. Freymann[4], Norio Komatsu[3,8,9], Marito Araki[3]*, Yoshikazu Tanaka[2]*, Ryuichi Sakai[1]*

*Corresponding authors. Email: Ryuichi Sakai <ryu.sakai@fish.hokudai.ac.jp>; Marito Araki <m-araki@juntendo.ac.jp>; Yoshikazu TANAKA <yoshikazu.tanaka@tohoku.ac.jp>

†These authors contributed equally to this work.

[1]*Graduate School of Fisheries Sciences, Hokkaido University; Hakodate, Japan.*

[2]*Graduate School of Life Sciences, Tohoku University; Sendai, Japan.*

[3]*Laboratory for the development of therapies against MPN, Juntendo University Graduate School of Medicine; Tokyo, Japan.*

[4]*Department of Biochemistry & Molecular Genetics, Feinberg School of Medicine, Northwestern University; Chicago, USA.*

[5]*Department of Physics, School of Science, Kitasato University; Sagamihara, Japan.*

[6]*Center for Disease Proteomics, School of Science, Kitasato University; Sagamihara, Japan.*

[7]*Graduate School of Integrated Sciences for Life, Hiroshima University; Higashi-Hiroshima, Japan*

[8]*Department of Advanced Hematology, Juntendo University Graduate School of Medicine; Tokyo, Japan.*

[9]*Department of Hematology, Juntendo University Graduate School of Medicine; Tokyo, Japan.*

One-sentence summary: A marine sponge lectin catalyzes thrombopoietin receptor dimerization and activation, exhibiting strong synergy with thrombopoietin, and modulates the internalization of the receptor.

Abstract

N-glycan-mediated activation of the thrombopoietin receptor (MPL) under pathological conditions has been implicated in myeloproliferative neoplasms induced by mutant calreticulin, which forms an endogenous receptor-agonist complex that constitutively activates the receptor. However, the molecular basis for this mechanism remains unstudied because no external agonist has been discovered. Here, we describe the structure and function of a marine sponge-derived MPL agonist, thrombocorticin (ThC). ThC-induced activation persists due to limited receptor internalization. Strong synergy between ThC and thrombopoietin suggests that ThC catalyzes the formation of receptor dimers on the cell surface. We show that MPL is subject to sugar-mediated activation and that lectin-mediated activation kinetics differ from cytokine-mediated activation kinetics. Our data demonstrated the potential of lectins to provide deeper insight into human pathogenesis.

Introduction

The thrombopoietin (TPO) receptor MPL plays critical roles in hematopoietic stem cell maintenance and platelet production (*1-3*). The activation of MPL that lacks kinase activity takes place by activation of Janus kinase 2 (JAK2) bound to the intracellular domain of MPL. The detailed process of receptor dimerization and activation of JAK2 by TPO, however, remains poorly defined, partly due to the lack of structural information on MPL (*4*). Under pathological conditions, myeloproliferative neoplasms (MPNs), mutant forms of glycan-dependent molecular chaperone CALR (CALRmut), bind to the immature sugar chain of MPL in the endoplasmic reticulum and then translocate to the cell membrane, forming a complex with functional MPL (*5-7*) and leading to the transformation of hematopoietic cells in an MPL-dependent manner (*8-10*). CALRmut activates MPL only in cells expressing CALRmut (*10, 11*), and the external agonist required for the recapitulation of this mode of activation has not been discovered, rendering assessment of the properties of lectin-type ligands for cytokine receptors difficult and leaving the molecular basis of this activation largely unstudied.

We recently identified a marine sponge-derived 14-kDa protein, thrombocorticin (ThC), as a potent agonist of MPL (*12*). Here, we report the three-dimensional structure of ThC as a novel fucose-binding lectin and the mechanisms underlying its MPL activation through binding to sugar chains on MPL.

Results

Biochemical profiles of ThC

We first identified a preliminary 131-amino acid sequence of native ThC (nThC) isolated from the sponge using mass spectrometry and Edman degradation after peptic digestion (Fig. 1A (i) and Fig. S1). A draft-ThC based on this sequence assigned lysine (K) to the 25th amino acid residue. Unlike nThC (*12*), however, draft-ThC failed to promote cell proliferation of Ba/F3-HuMpl, even at very high concentrations (Fig. 1B), leading to the conclusion that at least one amino acid residue in the draft-ThC sequence was assigned incorrectly. Therefore, we performed X-ray crystal structure analysis of n-ThC and found that the 25th amino acid residue originally assigned as K in the draft-ThC sequence was either glutamic acid (E) or glutamine (Q) (Fig. S2). Furthermore, an LC-MS/MS experiment unambiguously identified this residue as Q (Fig. S3). Upon these discoveries, the complete amino acid sequence of ThC was determined.

N-terminal His-tagged recombinant ThC (rThC) harboring Q at position 25 promoted the proliferation of Ba/F3-HuMpl cells (Fig. 1C) in an MPL-dependent manner (Fig. S4). Immunoblot analyses indicated that rThC activated steady-state JAK/STAT signaling (Figs. 1D and S4). These data indicated that rThC activates MPL to promote cell proliferation in Ba/F3-HuMpl cells.

Critical role of sugar-binding capacity in ThC-dependent MPL activation

The amino acid sequence of ThC shares approximately 33% identity with bacterial fucose-binding lectins; however, little similarity was found between ThC and TPO in both amino acid sequences (Fig. 1A (ii)) and three-dimensional structures (not shown). The activation of MPL by lectin-like molecules structurally distinct from TPO attracted our attention because CALRmut interaction with an immature sugar chain attached to the receptor in the course of receptor maturation was proposed as an alternative mode of MPL activation in pathological receptor activation in MPN (*5, 7*). We thus hypothesized that *ThC binds to sugar chains on the extracellular domain of the receptor on the cell surface, promoting MPL activation*. In agreement with this hypothesis, L-fucose or D-mannose inhibited ThC-dependent cell proliferation in Ba/F3-HuMpl cells (Fig. 2A). In contrast, the effects of the sugars on TPO-dependent cell proliferation were negligible (Fig. S6). The effects of fucose and mannose were concentration dependent, with half-maximal inhibitory concentration (IC_{50}) values of 22.7 and 6,676 μM, respectively (Fig. 2B). Subsequently, sugar

affinity column experiments showed that ThC bound to fucose and to mannose only in the presence of Ca^{2+} (Fig. 2C). Isothermal titration calorimetry (ITC) experiments confirmed Ca^{2+} dependence, with binding dissociation constants (KDs) of rThC bound to fucose or mannose in the presence of 5 mM Ca^{2+} of 4.72 and 66.2 x 10^{-6} M, respectively, consistent with the observations described above (Fig. 2D and Table S1). Taken together, these data implied that blocking ThC binding to MPL by sugar results in the inhibition of ThC-dependent cell proliferation.

Structural insights of ThC as a homodimeric lectin

To aid in the determination of the primary structure of ThC and to gain further structural insights into ThC itself, we determined the crystal structure of nThC at 1.6-Å resolution (Fig. 3). ThC has a β-sandwich structure composed of nine β-strands. An intramolecular disulfide bridge is formed between Cys3 and Cys111 (Fig. 3A), and two ThC molecules assemble as a homodimer in the crystal (Fig. 3A). This structural feature is shared with other fucose-binding lectins, *i.e.*, BC2 L-C-CTD and PA-IIL, which are homologous proteins of ThC, suggesting that dimeric assembly may be an important structural characteristic among them (Fig. S7). The structure of rThC superposed well on nThC (root-mean-square deviation (r.m.s.d.) of 0.66 Å for 261 Cα atoms), allowing us to consider it an equivalent molecule structurally and functionally to nThC; therefore, His-tagged rThC was used for further structural, physico-chemical, and physiological analyses, and it is termed ThC hereafter (Fig. S8). Structural insights into ThC, particularly the formation of homodimers, provide a rational model for MPL activation that is thought to be triggered by the homodimerization of receptor molecules.

Structural basis for ThC sugar binding

The crystal structure of ThC in complex with L-fucose (Fig. 3C) or D-mannose (Fig. S9) showed that the sugar molecule is bound in a cavity of the dimeric protein at the interface between two protomers via two Ca^{2+} ions, Ca-1 and Ca-2. Ca-1 was chelated in a polar cavity formed by D117-N119-D120 of one protomer and the C-terminal carboxylate of G131 of the other (denoted as Gly131*, Fig. 3C). This unique structural feature, herein called the 'pseudodomain-swapping motif', was formed between the protomers and is a characteristic hallmark of this protein family (Fig. 3D). Ca^{2+} was chelated by polar groups along the N107-D115-D117-D120 sequence (Fig. 3C). Sugar is recognized by ThC through polar interactions along the Ca-1-Ca-2-D115-D120-D108 sequence of one protomer and three hydroxy groups of the carbohydrates. Notably, the

pseudodomain-swapping structure enables stable carbohydrate binding through a hydrogen bond network established between the carboxylate of G131* of the adjacent protomer and Ca-1 and O4 of fucose (O2 of mannose). The positions of the carbohydrates were further stabilized by binding between O5 and Ser27 in both sugars. This manner of recognition shows the importance of Ca^{2+} in carbohydrate binding, which is consistent with the Ca^{2+} dependency of carbohydrate binding of ThC (Fig. 2C, D and Table S1). Stereochemical orientation of the three hydroxyl groups is shared in L-fucose and D-mannose but not the other chain-bearing sugars tested, explaining the carbohydrate specificity of ThC (Fig. S10). In the ITC analysis, a 1:1 stoichiometry between ThC and mannose/fucose was apparent (Fig. S11).

In the draft sequencing study of ThC, we coincidentally found that Q25 is a key residue for its agonist action (Fig. 1B). The ITC data showed a complete lack of affinity of Q25K (draft-ThC) for fucose (Fig. S11). To examine its structural basis, the Q25K mutant was crystallized in the presence of Ca^{2+}. In draft-ThC, the C-terminus faced away from Ca-1. The structure of draft-ThC clearly differed from that of nThC with respect to the conformation of the C-terminus in the counterpart protomer and the position of the side chain of Q25 (Fig. 3E). This conformational change caused the loss of the pseudointerprotomer swapping domain and, in turn, resulted in loss of Ca-1 coordination of the C-terminal carboxylate group of G131*, leading to profound loss of the fucose-binding capability and agonist activity of the mutant (Fig. 1B). We confirmed this series of changes by preparing a G132 mutant, in which an extra G residue was added to the C-terminus, with the intention of altering the pseudodomain-swapping motif. As expected, ITC analysis revealed that the G132 mutation diminished fucose-binding activity (Table S1 and Fig. S11), and agonist activity was completely lost (Fig. S12). These observations led to the identification of the structural determinants for the sugar-binding and agonist actions of ThC; specifically, the binding cavity of one protomer, two calcium ions, and the C-terminal domain of the other protomer together stabilize the sugar-bound state of the protein.

Activation of MPL by ThC via a fucosylated sugar chain

To gain further insight into the sugar-mediated activation of MPL, we assessed the effects of lectins bearing fucose- or mannose-binding properties on the proliferation of Ba/F3-HuMpl cells (Fig. 4A). All the lectins tested, except PA-IIL (*13*, *14*), a fucose-binding lectin homologous to ThC,

failed to promote the proliferation of Ba/F3-HuMpl cells. Despite the high degree of structural similarity between ThC and PA-IIL (r.m.s.d. 2.05 Å for 104 Cα atoms, Fig. S6), PA-IIL showed approximately 70-fold reduced potency in inducing MPL-dependent cell proliferation compared with ThC (Fig. 4B).

This result suggested that the dimerization and sugar specificity of a lectin alone are insufficient for an MPL agonist, although certain structural features inherent to ThC and PA-IIL contributed to their agonist action. Lack of agonist activity by BC2L-C-CTD, which belongs to the same family as PA-IIL (r.m.s.d. 1.18 and 2.13 Å for 111 and 106 Cα atoms with PA-IIL and ThC, respectively), strongly suggested that in addition to structural similarity, sugar-binding properties, specifically fucose binding, are crucial for MPL activation. The ITC data of PA-IIL and BC2L-C-CTD clearly showed that PA-IIL binds to both fucose and mannose (*15*), while BC2L-C-CTD binds only to mannose (Fig. S13). These data support the importance of fucose binding activity for MPL activation. Interestingly, however, MPL activation by PA-IIL was much weaker than that by ThC (Fig. 4B), even though the fucose binding affinity of PA-IIL was stronger than that of ThC (Table S1). Thus, we aimed to determine the inherent structural differences between the lectins by comparing the positions of two fucose molecules bound to ThC and PA-IIL. The distance between the representative atom of fucose O4 was 39.6 Å for ThC and 36.4 Å for PA-IIL (Fig. 4C). When one fucose molecule was superimposed, the position of the other was shifted by approximately 6.7 Å, such that the angle between three O4 atoms was 8.9 deg (Fig. 4C).

To demonstrate the importance of the fucosylated sugar chain, we treated Ba/F3-HuMpl cells with peracetylated 6-alkynyl fucose (6-Alk-Fuc), which is an inhibitor of *de novo* fucosylation enzymes (fucosyltransferases, FUTs) but can be internalized through the salvage pathway and added to the sugar chain (*16*); thus, fucose in the sugar chain is replaced by 6-Alk-Fuc. The resulting 6-Alk-Fuc Ba/F3-HuMpl cells were treated with ThC or TPO. 6-Alk-Fuc attenuated the cell proliferation by ThC and TPO with IC_{50} value of 1.2 and 5.0 μM, respectively, (Fig. 4D). These results indicated the considerable contribution of fucosylated glycans to receptor activation; however, the type of fucosylated chain with which ThC interacts could not be specified through an analysis of the aforementioned data alone. Human FUTs catalyze α(1,2)-, α(1,3)-, α(1,4)-, α(1,6)-, and *O*-fucosylation; thus, cell surface glycans may exhibit any of these fucosylation patterns (*17*). We

thus tested the effect of hypnin, an algal lectin with highly strict recognition for core α(1,6)-fucosylated glycans (*18*), on the action of ThC. We found that hypnin inhibited cell proliferation by ThC in a concentration-dependent manner with an IC_{50} of 5.88 μg/mL. Because the cytostatic concentration of hypnin was much higher (approximately 47 μg/mL, Fig. S14), the above result was ascribable to competitive inhibition between ThC and hypnin for core α(1,6)-fucose (Fig. 4E).

We next assessed the actions of ThC against glycan mutants of MPL. The extracellular domains of MPL have four consensus amino acid sequences for *N*-type glycans at N117, N178, N298, and N358 (*19*)(Fig. 4E). To determine the critical site for ThC activation, mutants in which N residues were replaced by Q residues were expressed in HEK293T cells, and receptor activation was monitored by the STAT5 reporter assay. The mutations did not significantly affect receptor activation by TPO (Fig. S15). In the case of ThC, however, differential activation between the mutants was apparent (Fig. 4E). Most strikingly, the N117Q mutant lost sensitivity completely. Next, three of four consensus N residues were replaced by Q residues, leaving only one glycan. Activation by ThC was significantly suppressed by these mutations; however, the mutant with N178/298/358Q, in which the N117 sugar remained, responded to the treatment. These data clearly supported the supposition that the TPO receptor can be activated through ligand binding at the surface glycan attached to the N117 residue of MPL.

Interestingly, the glycan site identified here is the same site that was previously attributed to activation by CALRmut under pathological conditions (*5-7, 20*). Because the property of CALRmut for MPL remains largely elusive due to a lack of an assay system (see above), we examined the mode of receptor activation induced by ThC. Unlike TPO that induced the activation of MPL in 10 min and resulted in a rapid attenuation of the activation, ThC activated MPL at 30 min after ligand addition and exhibited a capacity for the prolonged activation (Fig. 5A). When the levels of accumulated cell surface receptors were measured upon activation with a set of agonists, unlike the receptors in the TPO-treated cells, which were gradually decreased due to receptor internalization, the receptors remained on the cell surface in the ThC-treated cells (Fig. 5B). The signal activation and cell surface MPL levels showed a consistent decrease both in TPO and ThC. Prolonged accumulation of MPL on the cell surface was also observed in CALRmut-expressing cells, where receptor activation was persistent (*5*), as is the case for ThC cells. These observations led to the development of a new hypothesis that the mode of activation by lectin-type ligands is slow and steady but that of cytokine-mediated activation is rapid and extinctive.

Potentiation of TPO activity by lectins

Our observations strongly support the notion that *MPL can be activated by a mechanism completely different from that induced by currently known agonists*. Because lectin-type ligands likely maintain increased levels of receptors on the cell surface, we assessed whether such ligands synergize with natural ligands. For this purpose, we examined the concentration-dependent proliferation of TPO in Ba/F3-HuMpl cells in the presence of a subactivating concentration of ThC (0.1 μg/mL). As expected, ThC synergistically enhanced the agonist action of TPO (Fig. 5C). The rate of enhancement had a bell-shaped relationship with TPO concentration, showing that the effect was greatest when 0.2 ng/mL TPO was applied (Fig. 5C, lower tracing). At this concentration, TPO alone induced only a 10% increase in cell proliferation, which became 50% in the presence of ThC. The EC_{50} value (ng/mL) of TPO/ThC (0.27) was ten times lower than that of TPO (2.6). These data supported the idea that bidentate glycan-binding ligands may allosterically sensitize the action of TPO.

Discussion

Here, we determined the three-dimensional structure of the potent MPL agonist ThC as a homodimeric complex of lectin molecules featuring two calcium ions that form a cage-like complex for selective binding to fucose and mannose (Fig. 3C). We showed that ThC binds to fucose and, to a lesser extent, to mannose (Table S1) and demonstrated that the fucose binding property is critical for MPL activation (Fig. 4A, E). The mode of MPL activation by ThC resembles the pathogenic ligand CALRmut judged by the dependency of the N-glycosylation site on the activation (Fig. 4F) and by the persistent accumulation of receptor molecules on the cell surface (Fig. 5B). The lectin-type agonist promotes surface accumulation of cytokine receptors by blocking internalization (Fig. 5B) and induces slow but steady activation of downstream molecules (Fig. 5A), which can synergize with natural ligands (Fig. 5C). These data shed light on the previously understudied molecular mechanism of cytokine receptor activation by lectins.

This study presents the first evidence showing that an exogenous ligand activates MPL through surface glycans on the receptor. Most importantly, the glycan critical for the action of MPL is the same glycan that is required for MPL activation by CALRmut, an internal ligand (*5*, *7*). In cells expressing CALRmut, homomultimerized CALRmut engages with MPL bearing immature N-glycans at N117 in the endoplasmic reticulum (ER), seemingly forms the 2+2 quadripartite

complex of MPL-CALRmut in the Golgi apparatus, and is trafficked to the cell surface for activation (*5, 6, 21*). CALRmut fails to activate MPL expressed on the surface of cells that do not express CALRmut (*10, 11*), rendering the potential of CALRmut as the MPL ligand uncertain and leaving the molecular mechanism of MPL activation ambiguous. The present study clearly demonstrates that the N-glycan at N117 is the bona fide switch for the activation of MPL and ensures the agonistic effect of CALRmut on MPL.

Our structural insights into ThC led to the discovery of PA-IIL as a ThC-type MPL agonist, illustrating bacterial fucose-binding lectins, including theoretical lectins, as potential MPL agonists. The structural and biological comparison of ThC and PA-IIL implied that the dimerized form and the capacity of fucose binding were not sufficient for MPL activation. The position of MPL molecules, which is determined by positioning the fucose moiety at N117 of MPL bound by the lectin, plays a crucial role in the degree of receptor activation. Most strikingly, we found that the spatial arrangement of two fucose binding pockets differed clearly between ThC and PA-IIL. If the core-(1,6) fucose of sugar chain at N117 of each MPL binds tightly to two ligand binding cores of the lectin, configuration of the lectin-bound receptor complex may directly reflect the spatial relationship of the pocket; thus, ThC and PA-IIL-bound activating receptor complexes differ structurally. We propose that this structural difference affects the efficacies of the two lectins. A recent study demonstrated that dimeric antibodies that can bridge and dimerize MPL by binding various sites near the canonical ligand-binding domain of MPL can activate the receptor in distinctive ways; thus, agonist-based decoupling of self-renewal and differentiation was realized (*22*). Because no structural information on the 'active' receptor complex for MPL is known, the mechanistic basis of this phenomenon is elusive. However, our observation in conjunction with the above study supports the hypothesis that slight structural differences in the extracellular domain of MPL would affect receptor activation and possibly signaling.

Our results show that the ThC-dependent activation of MPL persists and is associated with the sustained expression of MPL on the cell surface. This was also observed in CALRmut-dependent MPL activation (*5*), implying a conserved mechanism of action in lectin-mediated receptor activation. The activation dynamics of MPL are largely controlled by internalization and recycling of the receptor as well as *de novo* biosynthesis of new receptors (*23*). Our results implied that internalization of ThC-activated receptors is a slow process, as observed in CALRmut-activated

receptors, giving rise to persistent activation. The strong synergy observed in the ThC/TPO co-application can be ascribed partly to sustained signaling by long-lasting cell surface receptors (Fig. S16).

MPL belongs to the class I cytokine receptor family, whose activation relies on the formation of receptor dimers; however, the process of dimer formation is not well understood (*24*). It has long been thought that preformed dimers are activated upon conformational alteration (*24, 25*). Recently, however, single-molecule live cell imaging of MPL expressed on HeLa cells revealed that the population of monomeric receptors surpasses that of the predimeric form and that the monomer assembles into dimers after interacting with agonists (*26*). Because we observed weak but sustained receptor activation by ThC associated with sustained cell surface expression of the receptor, we propose that a transition state, a *ligand-bound but subtle-activated dimer* in the process of signaling dimer formation, plays important roles (Fig. 5D III). The role of this well-conceivable transition complex formed in the middle of the activation process was previously hidden because this intermediate is short-lived in TPO-activated MPL due to potent 'native' interactions between the receptor and ligand. The strong synergy of ThC with TPO that we observed matches well with this hypothesis because predimerization facilitated by ThC largely reduces entropy during dimer formation. Thus, ThC can stabilize transition state III, although ThC-bound III eventually shifts to form signaling complex IV, presumably through the aid of intrinsic domain interactions in the transmembrane (TMD) and intracellular domains (Fig. 5D).

Because exogenously applied recombinant CALRmut fails to activate normal MPL (*10, 11*), ThC- and ThC-type fucose-binding lectins are the only probe, and they are excellent for studying the receptor kinetics and dynamics of MPL during activation through N-glycans. The present study is the first to disclose the structural basis of sugar-mediated activation of cytokine receptors. MPL-mediated signaling is involved in at least two discrete activation processes in hematopoiesis, namely, hematopoietic progenitor cell differentiation/megakaryocyte formation and hematopoietic stem cell self-renewal/maintenance (*1-3*). We propose that fucose-binding lectins are novel tools to control the structure of activating the MPL complex and enable fine-tuning of dimerization and internalization, as well as signaling in conjunction with co-application with other agonists. This line of experiments warrants a deeper understanding of MPL activation.

Acknowledgments

We thank Professor Yasuhiko Kizuka at Gifu University for providing 6-alkenyl fucose. We also thank Dr. Takanori Nakamura at Nissan Chemical Co. Ltd. for providing Ba/F3 cells; the Global Facility Center at Hokkaido University for performing amino acid sequence analysis; the Teijin Scholarship Foundation, Suntory Foundation for Life Sciences, and Japan Society for the Promotion of Science (JSPS) for the DC2 scholarship to H.W.; and the Chuuk State Department of Marine Resources for providing permission to collect sponges.

Funding

JSPS KAKENHI #19H03040, #21K08405, #19K08848
Ikeda Scientific Co., Ltd.
Grant-in-aid for JSPS fellows #20J11377
Takeda Science Foundation

Author contributions:

This work was conceptualized by H.W., R.S., M.A., and Y.T. H.N., T.O., T.M., Y.K., and H.W. analyzed the protein sequence. H.K., K.O., PJ.F., T.Y., T.O., D.F., and Y.T. overexpressed the proteins and analyzed their crystal structures and biochemical properties. N.M., M.A., and H.W. characterized the biological activities. K.H. and M.H. isolated hypnin. R.S., H.W., Y.T., M.A., and N.M. prepared the manuscript with input from all the other authors. N.K. supervised the study.

Competing interests: The authors declare that they have no competing interests.

References

1. A. Nakamura-Ishizu, T. Suda, Multifaceted roles of thrombopoietin in hematopoietic stem cell regulation. *Ann N Y Acad Sci* **1466**, 51-58 (2020).
2. K. Behrens, W. S. Alexander, Cytokine control of megakaryopoiesis. *Growth Factors* **36**, 89-103 (2018).
3. I. S. Hitchcock, K. Kaushansky, Thrombopoietin from beginning to end. *British journal of haematology* **165**, 259-268 (2014).
4. I. S. Hitchcock, M. Hafer, V. Sangkhae, J. A. Tucker, The thrombopoietin receptor: revisiting the master regulator of platelet production. *Platelets* **32**, 770-778 (2021).
5. N. Masubuchi *et al.*, Mutant calreticulin interacts with MPL in the secretion pathway for activation on the cell surface. *Leukemia* **34**, 499-509 (2020).
6. C. Pecquet *et al.*, Calreticulin mutants as oncogenic rogue chaperones for TpoR and traffic-

defective pathogenic TpoR mutants. *Blood* **133**, 2669-2681 (2019).

7. I. Chachoua *et al.*, Thrombopoietin receptor activation by myeloproliferative neoplasm associated calreticulin mutants. *Blood* **127**, 1325-1335 (2016).
8. C. Marty *et al.*, Calreticulin mutants in mice induce an MPL-dependent thrombocytosis with frequent progression to myelofibrosis. *Blood* **127**, 1317-1324 (2016).
9. S. Elf *et al.*, Mutant Calreticulin Requires Both Its Mutant C-terminus and the Thrombopoietin Receptor for Oncogenic Transformation. *Cancer Discov* **6**, 368-381 (2016).
10. M. Araki *et al.*, Activation of the thrombopoietin receptor by mutant calreticulin in CALR-mutant myeloproliferative neoplasms. *Blood* **127**, 1307-1316 (2016).
11. L. Han *et al.*, Calreticulin-mutant proteins induce megakaryocytic signaling to transform hematopoietic cells and undergo accelerated degradation and Golgi-mediated secretion. *J Hematol Oncol* **9**, 45 (2016).
12. H. Watari *et al.*, A novel sponge-derived protein thrombocorticin is a new agonist for thrombopoietin receptor. *Comp. Biochem. Physiol. C Toxicol. Pharmacol.* **221**, 82-88 (2019).
13. R. Loris, D. Tielker, K. E. Jaeger, L. Wyns, Structural basis of carbohydrate recognition by the lectin LecB from Pseudomonas aeruginosa. *J Mol Biol* **331**, 861-870 (2003).
14. E. Mitchell *et al.*, Structural basis for oligosaccharide-mediated adhesion of Pseudomonas aeruginosa in the lungs of cystic fibrosis patients. *Nat Struct Biol* **9**, 918-921 (2002).
15. C. Sabin *et al.*, Binding of different monosaccharides by lectin PA-IIL from Pseudomonas aeruginosa: thermodynamics data correlated with X-ray structures. *FEBS Lett* **580**, 982-987 (2006).
16. Y. Kizuka *et al.*, An Alkynyl-Fucose Halts Hepatoma Cell Migration and Invasion by Inhibiting GDP-Fucose-Synthesizing Enzyme FX, TSTA3. *Cell Chem Biol* **24**, 1467-1478 e1465 (2017).
17. J. Li, H. C. Hsu, J. D. Mountz, J. G. Allen, Unmasking Fucosylation: from Cell Adhesion to Immune System Regulation and Diseases. *Cell Chem Biol* **25**, 499-512 (2018).
18. S. Okuyama *et al.*, Strict binding specificity of small-sized lectins from the red alga Hypnea japonica for core (alpha1-6) fucosylated N-glycans. *Biosci Biotechnol Biochem* **73**, 912-920 (2009).
19. R. I. Albu, S. N. Constantinescu, Extracellular domain N-glycosylation controls human thrombopoietin receptor cell surface levels. *Front Endocrinol (Lausanne)* **2**, 71 (2011).
20. S. Elf *et al.*, Defining the requirements for the pathogenic interaction between mutant calreticulin and MPL in MPN. *Blood* **131**, 782-786 (2018).
21. M. Araki *et al.*, Homomultimerization of mutant calreticulin is a prerequisite for MPL binding and activation. *Leukemia* **33**, 122-131 (2019).
22. L. Cui *et al.*, Tuning MPL signaling to influence hematopoietic stem cell differentiation and inhibit essential thrombocythemia progenitors. *Proceedings of the National Academy of Sciences of the United States of America* **118**, (2021).
23. D. D. Dahlen, V. C. Broudy, J. G. Drachman, Internalization of the thrombopoietin receptor is regulated by 2 cytoplasmic motifs. *Blood* **102**, 102-108 (2003).
24. L. N. Varghese, J. P. Defour, C. Pecquet, S. N. Constantinescu, The Thrombopoietin Receptor: Structural Basis of Traffic and Activation by Ligand, Mutations, Agonists, and Mutated Calreticulin. *Front Endocrinol (Lausanne)* **8**, 59 (2017).
25. A. J. Brooks, M. J. Waters, The growth hormone receptor: mechanism of activation and clinical implications. *Nat Rev Endocrinol* **6**, 515-525 (2010).

26. S. Wilmes *et al.*, Mechanism of homodimeric cytokine receptor activation and dysregulation by oncogenic mutations. *Science* **367**, 643-652 (2020).

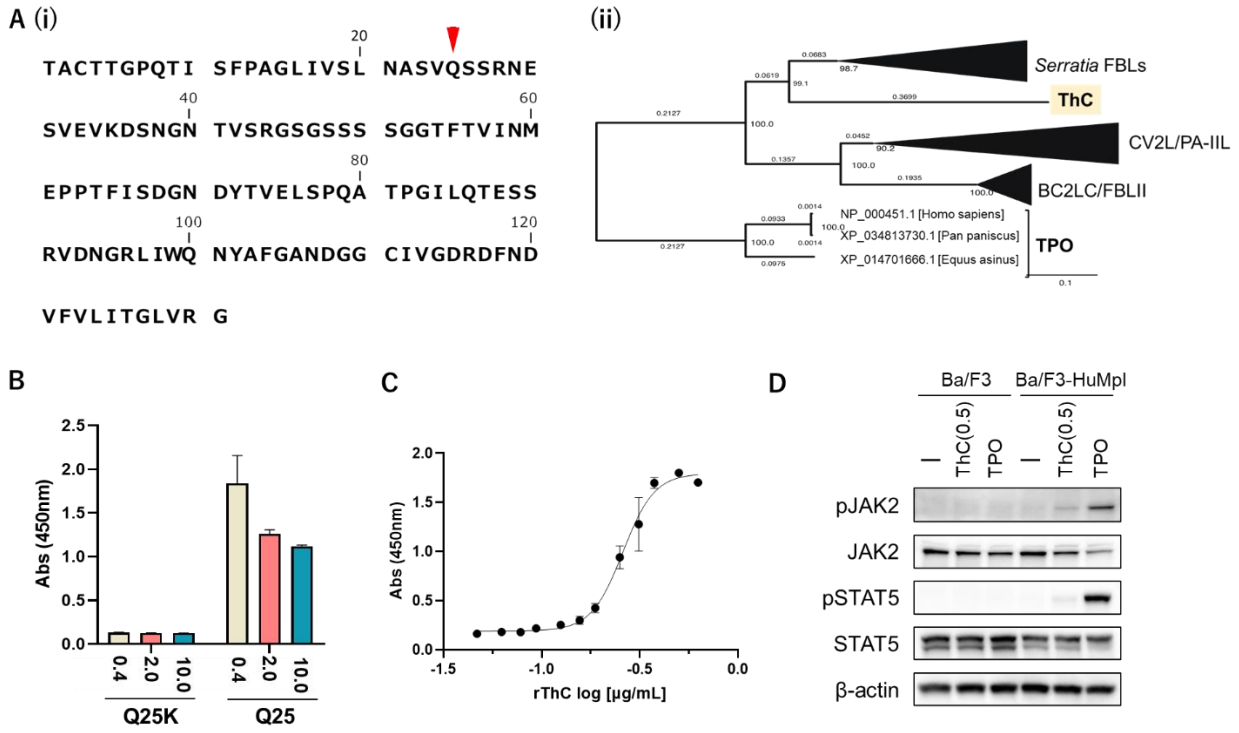

Fig. 1. Biochemical profiles of ThC.

(A) (i) Amino acid sequences of ThC. The red arrowhead indicates the Q residue at position 25, which was assigned as K in the draft sequence. (ii) Phylogenetic tree of ThC, related bacterial lectins and TPO with collapsed tree nodes (Fig. S5). (B) A comparison of the activity of rThC (Q25) and the Q25K mutant in Ba/F3-HuMpl cell proliferation. (C) Concentration-response curve of proliferating Ba/F3-HuMpl cells by rThC. The half-maximal effective concentration EC_{50} was 0.26 and 0.31 μg/mL for the recombinant ThC and nThC (*12*), respectively. (D) Immunoblot analysis of Ba/F3 and Ba/F3-HuMpl cells upon steady-state activation by TPO and rThC.

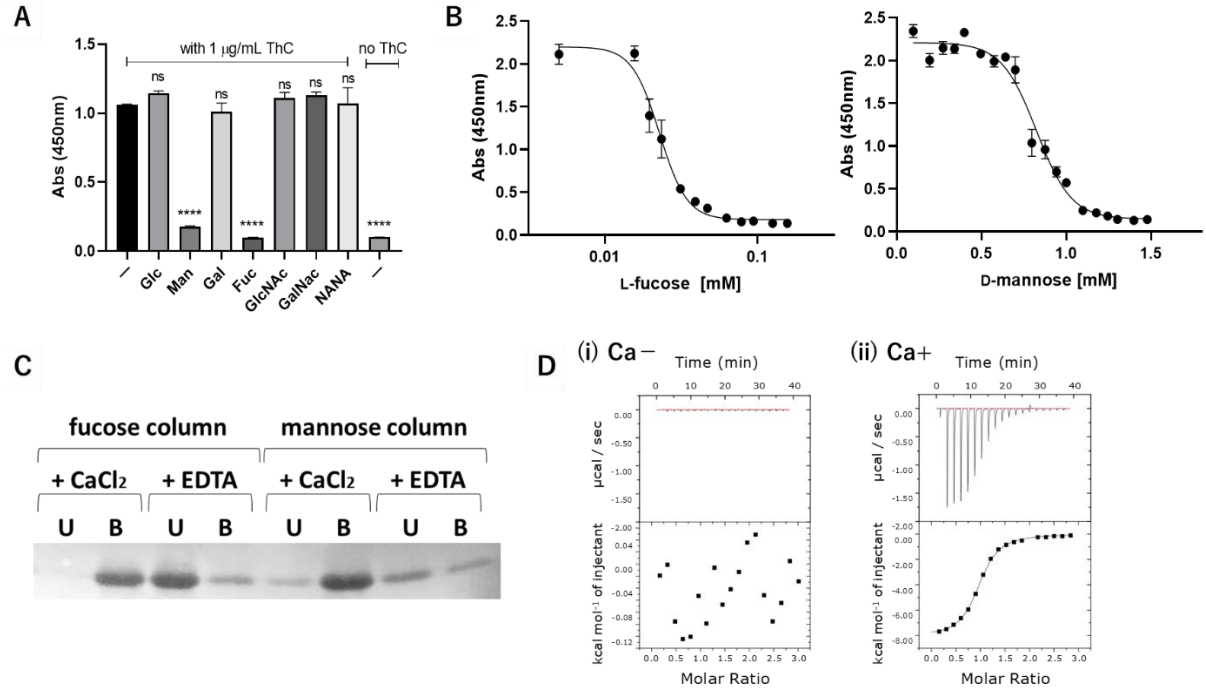

Fig. 2. Critical role of sugar-binding capacity in ThC-dependent MPL activation.
(A) Relative cell proliferation in the presence of various sugars (10 mM) in Ba/F3-HuMpl cells with rThC (1 μg/mL). ****P < 0.001, ns, not significant. (B) Concentration-dependent inhibition of fucose or mannose upon cell proliferation by rThC treatment (1 μg/mL). (C) Binding capacity of rThC to fucose- or mannose-immobilizing resins in the presence of 1 mM $CaCl_2$ or 1 mM EDTA. Unbound (U) and bound (B) rThC to the resin is shown as a pair. (D) Thermodynamic analysis by ITC of the interaction with fucose in the absence (left) and presence (right) of 1 mM $CaCl_2$. Thermogram (top) and titration curve (bottom) are shown.

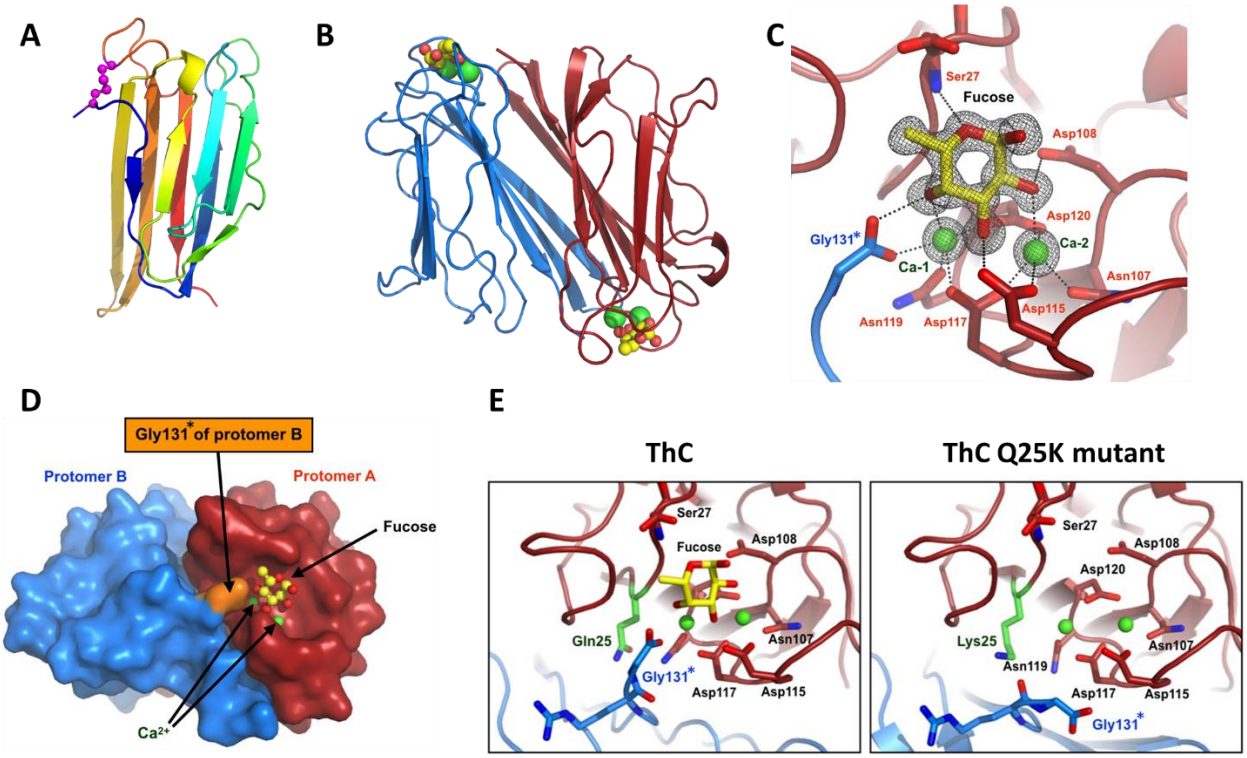

Fig. 3. Crystal structure of ThC.

(A) Ribbon diagram of the nThC monomer colored according to the sequence in blue at the N-terminus to red at the C-terminus. The disulfide bond between Cys3 and Cys111 is shown as a magenta ball. (B) Dimer structure of rThC in complex with Ca^{2+} (green ball) and fucose (ball-and-stick model, yellow: carbon, red: oxygen). (C) A close-up view of the fucose binding site of rThC. The bound Ca^{2+} ions and fucose are shown as green balls and stick models, respectively. Residues are colored according to the chain as in (B). A Fo-Fc map of the fucose and Ca^{2+} is shown. (D) Pseudodomain swapping structure in dimeric rThC. Gly 131*, shown in orange, of one protomer intervenes in the other. (E) Structure comparison of the Ca^{2+} binding configuration between wild type (left) and Q25K (right). Close-up view of the fucose binding site is shown. Individual protomers are shown in red and blue. The substituted residue (N25 and K25) is shown in green.

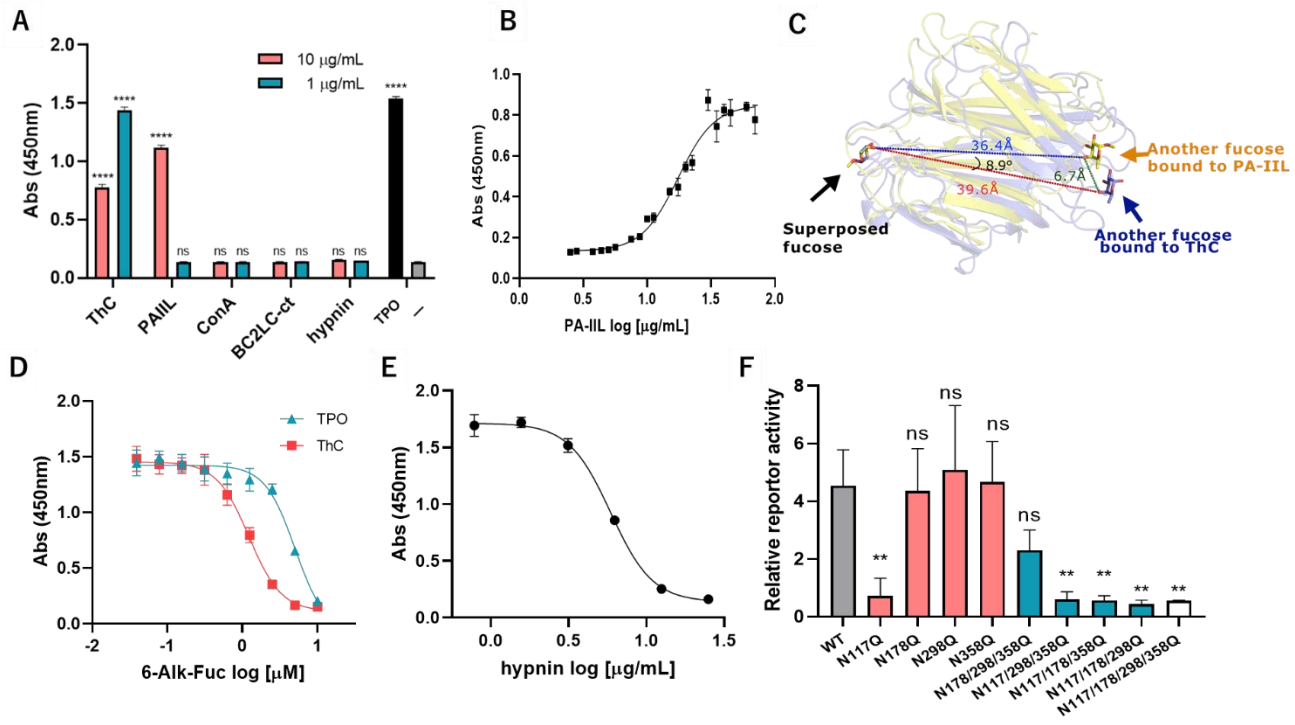

Fig. 4. Involvement of the fucose moiety in ThC-dependent MPL activation.

(A) Effect of lectins on the proliferation of Ba/F3-HuMpl cells: PA-IIL, a fucose/mannose selective bacterial lectin with high homology to ThC; ConA, a mannose specific legume lectin; BC2 L-C-CTD, mannose-selective bacterial lectin with high homology to ThC; hypnin, a core 1,6-fucosylated glycan-specific algal lectin. TPO, 10 ng/mL; (-), no agonist. (B) Concentration dependency of Ba/F3-HuMpl cell proliferation induced by PA-IIL (EC_{50} = 17.5 μg/mL). (C) Relative positions of two fucose molecules bound to the ThC dimer and PA-IIL dimer. One of the two fucose molecules bound to each is superimposed (fucose on the left). The other fucose molecule is shown as sticks. Purple represents the fucose bound to ThC, and yellow represents the fucose bound to PA-IIL. The numbers represent the distance between O4 atoms (red: between two fucoses of ThC, blue: between two fucoses of PA-IIL, green: between fucoses of ThC and PA-IIL) and the angle between the three O4s of superimposed fucoses, that of PA-IIL bound fucose, and that of ThC bound fucose. Ribbon diagrams of the ThC dimer (purple) and PA-IIL dimer (yellow) are also shown in translucent form. (D) 6-alkynyl-fucose mediated inhibition of cell proliferation induced by ThC (1 μg/mL) and TPO (10 ng/mL). (E) Hypnin-mediated inhibition of cell proliferation induced by ThC (1 μg/mL) with an IC_{50} value of 5.88 μg/mL. (F) Effect of mutations on potential N-glycosylation sites on MPL for activation by ThC (1 μg/mL). STAT5 reporter activity representing MPL activation status was measured and is depicted. Gray bar: wild-type (WT) MPL; red bars: single-site mutant MPL; blue bars: triple-site mutant MPL; and white bar: quadruple-site mutant MPL. $^{**}P < 0.01$, $^{****}P < 0.001$, ns: not significant.

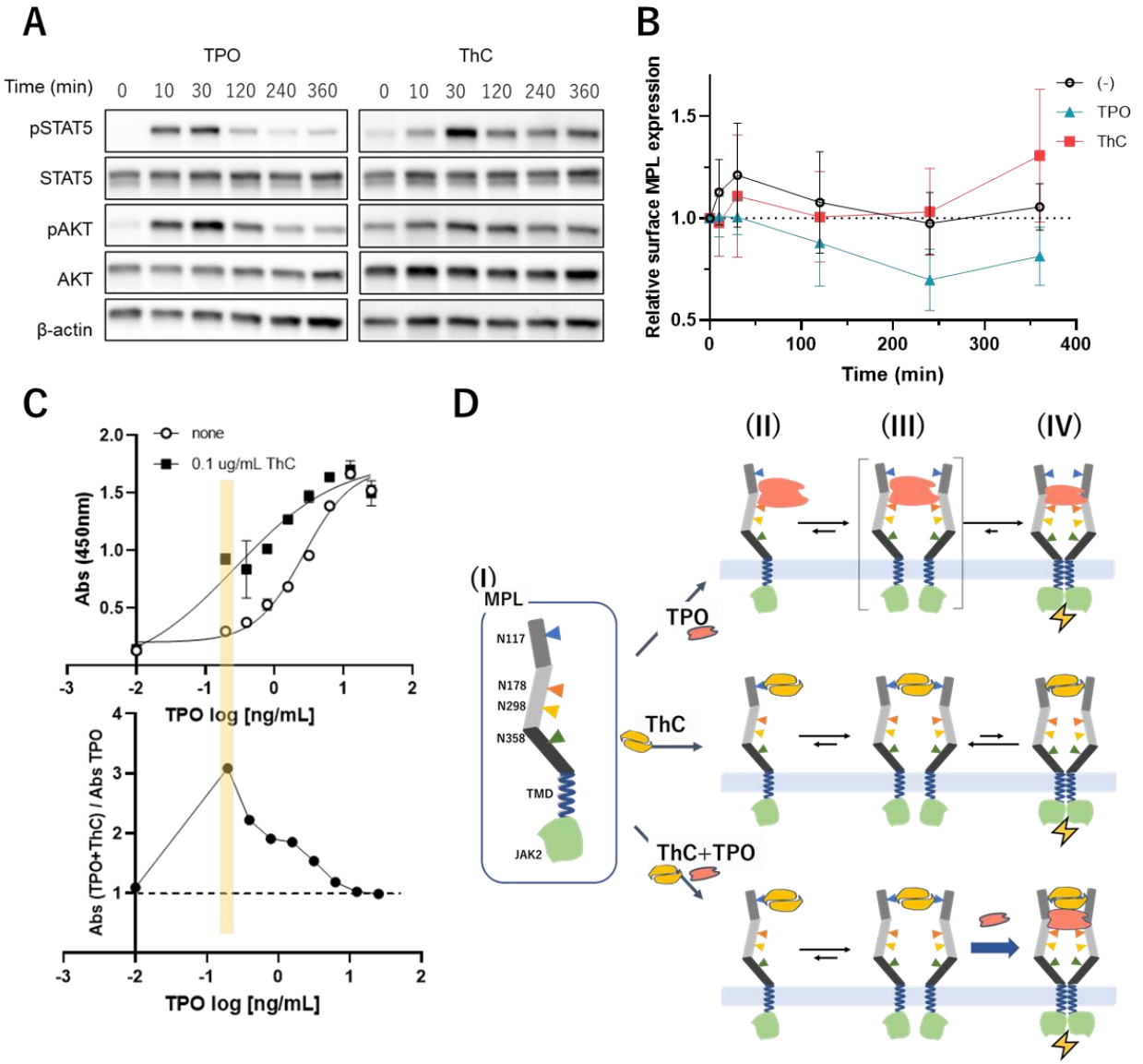

Fig. 5. Differential processes of MPL activation.

(A) Time-dependent activation of MPL-downstream molecules in Ba/F3-HuMpl cells treated with ThC (1 μg/mL) and TPO (3 ng/mL). Phosphorylation of STAT5 and AKT was monitored at the indicated times after the addition of an agonist(B) Relative amount of MPL on the cell surface. 0, 10, 30, 120, 240, and 360 min after the addition of ThC (1 μg/mL) and TPO (3 ng/mL).

(C) Synergic effects observed in a given combination of agonists in the Ba/F3-HuMpl cell proliferation assay. Concentration-response curve for tested agonists in the absence or presence of fixed subactivation concentrations of ThC (0.1 μg/mL) (upper trace). The ratios of absorptions with and without ThC (0.1 μg/mL) are plotted (lower trace).(D) Proposed mechanisms for activation by two mechanistically discrete agonists, TPO and ThC: (I) Schematic depiction of MPL. Monomeric MPL has four N-glycosylation sites at N117, 178, 298, and 358; (II) ligand-bound monomeric state with each TPO and ThC; (III) ligand-bound nonactivated state; (IV) dimeric signaling complexes. (D) Synergic activation by basal subactivation concentrations of ThC and TPO.